



ELSEVIER

Available online at [www.sciencedirect.com](http://www.sciencedirect.com)

SCIENCE @ DIRECT®

Physics Letters A 318 (2003) 251–269

PHYSICS LETTERS A

[www.elsevier.com/locate/pla](http://www.elsevier.com/locate/pla)

# Tidal effects in space experiments to test the equivalence principle: implications on the experiment design

G.L. Comandi<sup>a</sup>, A.M. Nobili<sup>a,b,\*</sup>, R. Toncelli<sup>a,b</sup>, M.L. Chiofalo<sup>a,b</sup>

<sup>a</sup> *Space Mechanics Group, Department of Mathematics, University of Pisa, Via F. Buonarroti, I-56127 Pisa, Italy*

<sup>b</sup> *INFN, Sezione di Pisa, Via F. Buonarroti, I-56127 Pisa, Italy*

Received 10 June 2003; accepted 30 July 2003

Communicated by V.M. Agranovich

## Abstract

Experiments to test the equivalence principle (EP) in low Earth orbit require to detect the effects of an extremely small non-classical differential acceleration between test masses of different composition. In all proposed experiments the test masses are concentric coaxial cylinders, so as to reduce classical tidal effects which are differential too. Perfect centring being impossible, tidal effects need to be carefully investigated as they impose severe constraints on the basic features of the experiment design. The present analysis shows that with free flying (uncoupled) test masses an EP violation signal could be detected if the initial conditions of the masses were finely adjusted for them to remain at a fixed distance relative to each other while orbiting around the Earth. However, such an experiment is severely limited by non-gravitational effects. If the test cylinders are weakly coupled in 2D in the plane perpendicular to their symmetry axis (close to the orbit plane), while rapidly spinning around it, a position of relative equilibrium is provided by physical laws which makes tidal effects widely separated from the signal. Weak coupling in 1D along the symmetry axis (to lie and slowly rotate in the orbit plane) is viable but less advantageous.

© 2003 Published by Elsevier B.V.

*Keywords:* Equivalence principle; Tidal effects; Rotordynamics

## 1. Introduction

The equivalence principle (EP) is tested through its most direct consequence, the universality of free fall (UFF), whereby in a gravitational field all bodies fall the same regardless of their mass or composition. UFF experiments therefore require two test masses in the gravitational field of a source body plus a read-out system to detect the effects of tiny, non-classical differential forces acting between the two. If the experiment is carried out with the test masses enclosed by a spacecraft orbiting the Earth at low altitude the driving signal is much stronger than it is for suspended bodies on the surface of the Earth. However, unless the centers of mass of the orbiting bodies are perfectly coincident, classical (differential) tidal effects arise which might compete with a non-classical EP

\* Corresponding author.

*E-mail address:* [nobili@dm.unipi.it](mailto:nobili@dm.unipi.it) (A.M. Nobili).

violation signal. This is why in all proposed EP experiments in space the test masses are “concentric” coaxial cylinders [1–3]. However, since perfect centering is impossible to achieve, the signature and amplitude of tidal effects must be carefully assessed, as they might compete directly with the target signal of a putative EP violation. For the space missions under study the goals are to perform an EP test to:  $10^{-15}$  with  $\mu$ SCOPE [3],  $10^{-17}$  with “Galileo Galilei” (GG) [1],  $10^{-18}$  with STEP [2].

We proceed by investigating, using analytical as well as numerical methods, different model cases of increasing complexity. We start in Section 2 with the case of free flying (uncoupled) test masses, showing that tidal effects and EP violation signal have the same frequencies. For the relative displacement of an EP violation to be detected with certainty the initial conditions of the bodies should be adjusted so that they orbit the Earth with the same mean angular velocity while remaining fixed relative to each other. Non-gravitational effects due to electric charging of the test masses make it very hard to realize this configuration.

In Section 3 we demonstrate that one way to separate the EP violation signal from the tide is to couple the test masses in the orbit plane, e.g., with a mechanical spring, thus introducing a natural frequency of differential oscillation of the test masses with respect to one another. In this case, while the EP signal is still detected at the orbital frequency, tides are at the natural differential frequency, and at this frequency plus or minus twice the orbital frequency. This is the case of the proposed “Galileo Galilei-GG” space experiment, where the natural differential frequency is about a factor 10 away from the orbital frequency, which makes it easy to separate tidal effects from the signal. The need for all EP experiments in space to spin the spacecraft in order to provide a frequency modulation of the signal is discussed in Section 4. In Section 5 the GG experiment is analysed under realistic conditions, including the rotation of the system in super-critical regime, to demonstrate that indeed an EP violation signal would not be masked by tidal effects. While the well-known self-centring property of super-critical rotors is exploited in GG, this is not possible in the STEP and  $\mu$ SCOPE experiments discussed in Section 6 because the test bodies are constrained to 1D motion. Being in sub-critical regime, they would then be too much off-centred at equilibrium, which makes it necessary to actively force their centres of mass as close as possible to each other. The masses are actively maintained in their fixed position and the force required to do that is the observable from which a possible signal of violation should be extracted. In this case tidal effects are at twice the orbital/EP-violation-signal frequency (i.e., they are separated by a factor 2), and they are larger than the signal because of the difficulties of active centring. Overall this design is less elegant and advantageous than the GG design, the main issue being that the masses do not rotate around their symmetry axis.

## 2. EP violation signal and tidal effects on free-flying test masses in low Earth orbit

If two test masses of different composition, falling in the gravitational field of the Earth with an acceleration  $a$  and the same initial conditions, experience a non-classical differential acceleration  $\Delta a$  it means that there is an EP violation to the level  $\eta = \Delta a/a$ . However, exactly the same differential acceleration might be due to a difference  $\Delta r$  in the orbital distance  $r$  of the two bodies at initial time such that  $\Delta r/r \simeq \Delta a/a$ , with no EP violation. We demonstrate this fact by analyzing the case of an initial separation  $\Delta r$  and no violation (case (i)), and then the case with a violation to the level  $\eta$  and zero initial separation (case (ii)). We investigate also an ideal experiment configuration such that, having reached appropriate initial conditions, the test masses remain fixed with respect to each other while freely orbiting the Earth. Then, by measuring their fixed relative displacement it should be possible to tell if there is an EP violation or not. Non-gravitational effects appear to be a major limitation to achieving and maintaining such fixed configuration.

### 2.1. Test masses separated by $\Delta r$ ; no EP violation (case (i))

In absence of EP violation inertial and gravitational mass are the same. Body 1, with mass  $m_1^i = m_1^g \ll M_\oplus$ , starts its motion around the Earth at an orbital distance  $r_1(0) = r$  and with the corresponding Keplerian velocity

$v_1(0) = \sqrt{GM_\oplus/r}$  perpendicular to its position vector, whereas body 2, with mass  $m_2^i = m_2^g \ll M_\oplus$ , is released at  $r_2(0) = r + \Delta r$  with  $\vec{v}_2(0) = \vec{v}_1(0)$ . Therefore, while body 1 performs a circular orbit with constant angular velocity (mean motion)  $n_1 = n_1(0) = \sqrt{GM_\oplus/r^3}$ , body 2 moves along an elliptic orbit with major semiaxis  $a$  and eccentricity  $e$  satisfying the relationship:

$$a(1 - e) = r + \Delta r. \quad (1)$$

Referring to Appendix A for details, we obtain

$$\Delta n \equiv n_2 - n_1 \simeq -n_1 \cdot \frac{3\Delta r}{r} \quad (2)$$

for the relative mean motion of the two bodies. Since the orbital periods  $P_1 = 2\pi/n_1$  and  $P_2 = 2\pi/n_2$  are slightly different, the bodies' separation in longitude around the Earth will grow with time.

We have computed the time-evolution of the relative positions  $X \equiv x_1 - x_2$  and  $Y \equiv y_1 - y_2$  of the two bodies, by numerically integrating the equations of motion

$$m_\alpha^i \ddot{x}_\alpha = -\frac{GM_\oplus m_\alpha^g x_\alpha}{(x_\alpha^2 + y_\alpha^2)^{3/2}}, \quad m_\alpha^i \ddot{y}_\alpha = -\frac{GM_\oplus m_\alpha^g y_\alpha}{(x_\alpha^2 + y_\alpha^2)^{3/2}} \quad (3)$$

with  $m_\alpha^i = m_\alpha^g$  and  $\alpha = 1, 2$ . The orbit of body 2 relative to body 1 is shown in Fig. 1. It is a spiral, and the relative distance grows with time at the orbital frequency.

## 2.2. Test masses with the same initial conditions but with an EP violation $\eta$ (case (ii))

Body 1 and body 2 start their motion with identical initial conditions, namely, at distance  $r_1(0) = r_2(0) = r$  with initial velocity  $v_1(0) = v_2(0) = \sqrt{GM_\oplus/r}$  along the tangential direction. In this case though, there is an EP violation  $\eta$  such that:

$$m_2^g = m_2^i(1 + \eta). \quad (4)$$

Thus, while the equations of motion for body 1 is the same as (3), those for body 2 are modified into

$$m_2^i \ddot{x}_2 = -\frac{Gm_2^i(1 + \eta)x_2}{(x_2^2 + y_2^2)^{3/2}}, \quad m_2^i \ddot{y}_2 = -\frac{Gm_2^i(1 + \eta)y_2}{(x_2^2 + y_2^2)^{3/2}}. \quad (5)$$

As a result, to first order in  $\eta$  the Keplerian elements  $a$  and  $e$  of orbit 2 and the difference  $\Delta n$  in mean motion are (see Appendix B):

$$e \simeq -\eta, \quad a \simeq r(1 - \eta), \quad \Delta n \simeq 2\eta. \quad (6)$$

Again, since the orbital periods of the two bodies are slightly different, the motion of body 2 relative to body 1 is a spiral, but in this case it starts from the origin. By comparing the expressions for  $\Delta n$  in (6) and in (2), it turns out that under the condition:

$$\eta = -\frac{3}{2} \frac{\Delta r}{r} \quad (7)$$

the relative orbit resulting from the classical tidal effect of case (i) and the one with an EP violation of case (ii) grow at the same rate. This is shown in Fig. 2, while Fig. 3 shows that the dominant frequency in the relative displacement of the test cylinders is the orbital one, both in the classical case with tides and in the non-classical case with an EP violation (with relation (7) between  $\Delta r$  and  $\eta$ ).

Case (i) represents a space-fixed-like configuration. We now consider the case in which the two bodies have the same initial angular velocity  $n_1 = n_2 = \sqrt{GM_\oplus/r^3}$  but they are released at different altitudes (Earth-pointing-like

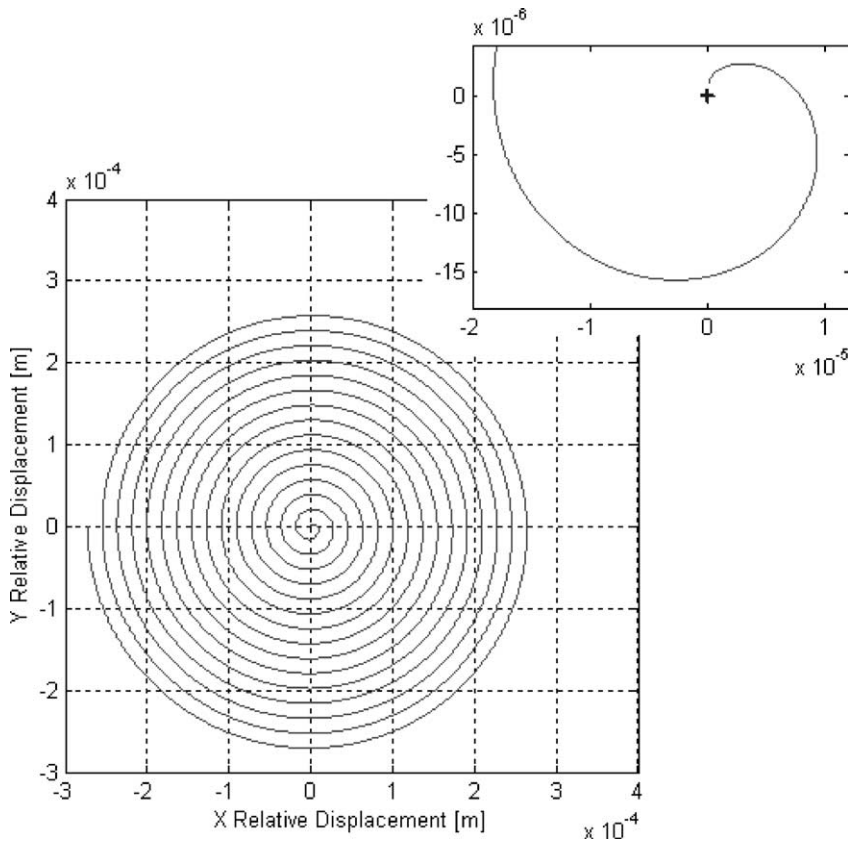


Fig. 1. Case (i): test bodies with initial separation  $\Delta r$  and no EP violation. Orbit of body 2 relative to body 1 for 15 orbital periods having taken  $\Delta r = 1 \times 10^{-6}$  m and  $r = R_{\oplus} + h$  with  $h = 500$  km. Inset: close-up of the relative motion in the first half period.

configuration). The initial conditions for body 1 being the same, for body 2 we take:

$$r_2(0) = r + \Delta r, \quad v_2(0) = n_1(r + \Delta r). \tag{8}$$

The difference in mean motions in this case is (see Appendix C for details):

$$\Delta n \simeq -n_1 \cdot \frac{6\Delta r}{r}. \tag{9}$$

The motion of body 2 relative to body 1 in the Earth-pointing case is quite similar to that of the space-fixed configuration, the only difference being that the relative distance grows twice as fast. Again, the initial separation  $\Delta r$  mimics an EP violation if

$$\eta = -3 \frac{\Delta r}{r}. \tag{10}$$

Expression (10) differs from (7) by the same factor of 2. In any case, the value  $\Delta r$  of the release error of the test masses which would result in a classical effect as large as the targets of the proposed missions is of the order of a nanometer for the least ambitious goal of  $\mu$ SCOPE, and even smaller (to the level of a few tens of picometers or just several picometers in GG and STEP). Release errors as small as these are impossible to achieve. The uncertainty with which initial conditions (and the orbital elements) can be determined would set the limiting sensitivity in EP testing with these experiments. The same conclusion is reported in [4,5]. How is it possible, then, that lunar

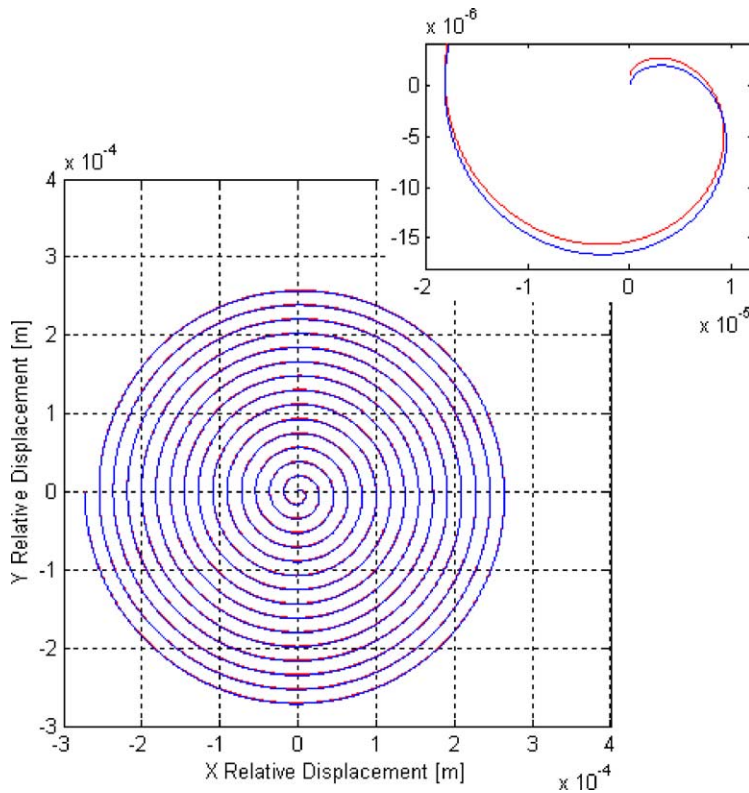


Fig. 2. (Figure is in colour on the web.) Blue curve: orbit of body 2 relative to body 1 for  $\eta = 2.1 \times 10^{-13}$  after  $15P_1$  of integration time (case (ii): identical initial conditions in the presence of an EP violation). The classical orbit of case (i) with  $\Delta r = -2r\eta/3 = 10^{-6}$  m is shown as a red curve for comparison. The value of  $r$  is the same as in Fig. 1.

laser ranging (LLR) data can be used to search for EP violations in the Earth–Moon–Sun system of free masses by checking whether the Earth and the Moon fall the same in the gravitational field of the Sun? LLR tests of the equivalence principle have been able to reach  $\eta_{\text{LLR}} \simeq 10^{-13}$  [6] because at this level, at the 1 AU orbital distance of the Earth–Moon system from the Sun,  $\Delta r$  must of the order of a few mm, which is just in the present capabilities of current lunar laser tracking technology.

### 2.3. An ideal EP experiment with free falling test masses

In order to avoid the spiral motion of Figs. 1 and 2, it is possible in principle to adjust the initial conditions of the test bodies so that their relative position vector remains fixed with respect to the centre of the Earth while orbiting around it (i.e., the test bodies must have the same orbital angular velocity). Then, by measuring their separation distance it would be possible to tell whether there is an EP violation or not: if there is a non-zero separation vector  $\Delta \vec{r}$  pointing to the center of the Earth, and in addition the masses remain fixed with respect to each other (no motion along track), this means that there is an EP violation to the level  $\eta \simeq \Delta r/r$  (provided that the motion is dominated by gravity). The experiment requires: first to be able to reach the initial conditions which make the test masses orbit the Earth in a fixed configuration; then to measure their relative displacement; and finally to make sure that there is no relative motion along track due to gravitation. The first step appears to be the most difficult one because of the electrostatic effects caused by the well-known phenomenon of electric charging of the test masses (note also that charging changes with time in an unpredictable way). As for checking that there is no relative motion along

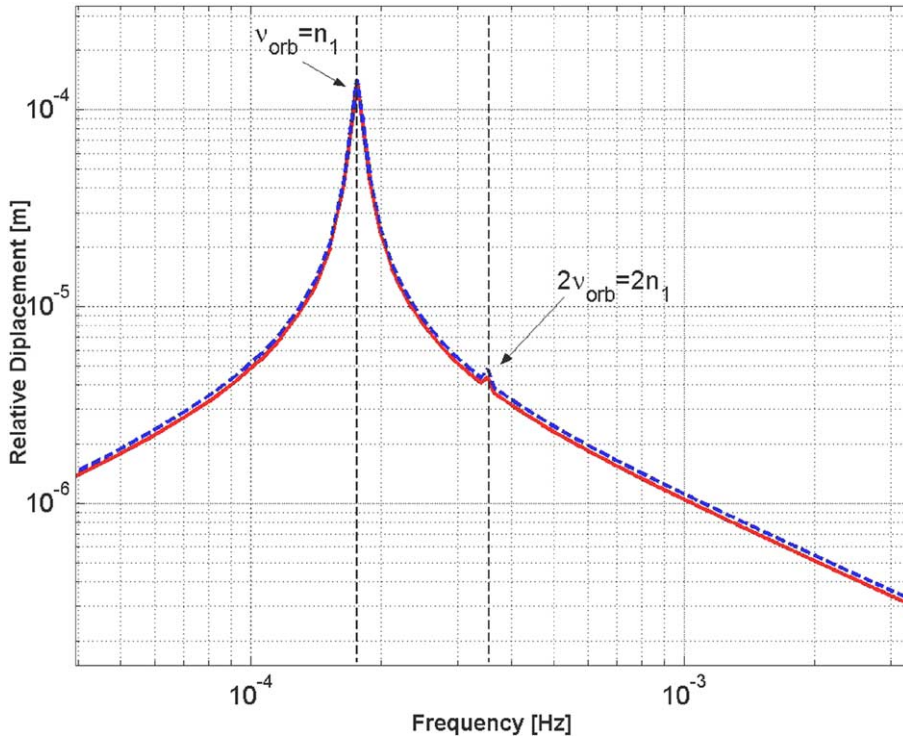


Fig. 3. FFT of the signals in the inertial reference frame. Solid curve: the orbit corresponding to case (ii) of two bodies starting with identical initial conditions in the presence of an EP violation. The orbit corresponding to case (i) with  $\Delta r = -2r\eta/3 = 10^{-6}$  m is shown as a dashed curve for comparison. In the inertial reference frame, the tidal effect and EP signal would be detected at  $\nu_{\text{orb}}$  and  $2\nu_{\text{orb}}$ . The main contribution is at the orbital frequency.

track, this might be difficult because of the competing effect of residual air drag along the orbit of the satellite, whose effect is a linear displacement growing quadratically with time. If the test masses are free flying air drag on the spacecraft gives rise to the same inertial acceleration on both test masses (common mode); however, a residual differential displacement is detected by the read out if the common mode one is much larger than the target signal. Drag compensation is needed, and can be realized, but the problem remains of how to separate with certainty an along track motion of pure gravitational origin whose presence in this experiment would rule out EP violation. We conclude that an EP experiment in space with free falling, uncoupled, test masses would have to face severe limitations.

### 3. EP violation signal and tidal effects with test masses coupled in the orbit plane

We now show that if the test bodies are coupled in the orbit plane, tidal effects and EP violation signal appear at different frequencies, which makes it possible to separate them out. Let us consider a spacecraft orbiting the Earth with radius  $r$  and Keplerian angular velocity

$$\omega_{\text{orb}} = \sqrt{\frac{GM}{r^3}}. \quad (11)$$

Let the test masses  $m_1$  and  $m_2$  be separated by  $\Delta r$  in their initial orbital distance, and be coupled to each other with a positive stiffness  $k$  (the coupling may be of different nature, e.g., mechanical, electrostatic or magnetic) in

the orbit plane. The suspension is assumed to be rigid (in reality it is only much stiffer) along the orbit normal. We investigate their motion in the reference frame of the orbiting satellite. The frame is centered on the center of mass of the Earth, with the  $x$  axis in the Earth-to-satellite direction, the  $z$  axis perpendicular to the orbit plane and the  $y$  axis to complete the Cartesian system. In this frame we call  $\vec{r}_1$  and  $\vec{r}_2$  the test masses position vectors with respect to the center of mass of the spacecraft, and  $\vec{\rho}_1 = \vec{r} + \vec{r}_1$ ,  $\vec{\rho}_2 = \vec{r} + \vec{r}_2$  their position vectors with respect to the center of mass of the Earth. The bodies have the same inertial mass but different composition. In addition it is assumed that there is a violation of the equivalence principle to the level  $\eta$ , namely:  $m_1^i = m_2^i \equiv m$  and  $m_1^g = m$ ,  $m_2^g = m(1 + \eta)$ . The Lagrange function is:

$$L = \frac{1}{2}m[\dot{r}_{1x}^2 + \dot{r}_{1y}^2 + 3\omega_{\text{orb}}^2 r_{1x}^2 + \omega_{\text{orb}}(r_{1x}\dot{r}_{1y} - r_{1y}\dot{r}_{1x}) + \dot{r}_{2x}^2 + \dot{r}_{2y}^2 + 3\omega_{\text{orb}}^2 r_{2x}^2 + \omega_{\text{orb}}(r_{2x}\dot{r}_{2y} - r_{2y}\dot{r}_{2x})] - \frac{1}{2}k(r_{1x}^2 + r_{1y}^2 + r_{2x}^2 + r_{2y}^2 - 2r_{1x}r_{2x} - 2r_{1y}r_{2y}) - m\omega_0^2 r \eta r_{2x} + \frac{1}{2}m\omega_0^2 \eta (2r_{2x}^2 - r_{2y}^2). \quad (12)$$

Tidal effects can be singled out by putting  $\eta = 0$  in (12) (i.e., no EP violation), and then deriving the equations of motion of the test masses in their relative coordinates  $X = r_{2x} - r_{1x}$  and  $Y = r_{2y} - r_{1y}$ :

$$\begin{cases} \ddot{X} - 2\omega_{\text{orb}}\dot{Y} + (\omega_n^2 - 3\omega_{\text{orb}}^2)X = 0, \\ \ddot{Y} + 2\omega_{\text{orb}}\dot{X} + \omega_n^2 Y = 0. \end{cases} \quad (13)$$

The angular frequency  $\omega_n = \sqrt{2k/m}$  appearing in (13) is the natural frequency of oscillation of the test masses relative to one another in the orbit plane due to the coupling stiffness  $k$ : the weaker the coupling stiffness, the more sensitive the test bodies are to differential forces, such as those due to tides or EP violation. In space, thanks to weightlessness, the coupling can be very weak, much weaker than on the ground where suspensions must be stiff enough to withstand local gravity. Hence, the natural differential frequency can be much lower in space than in the lab. Yet, it is always much larger than the orbital frequency, which in all proposed space experiments is about  $1.7 \times 10^{-4}$  Hz (typical orbital periods in low Earth orbit are 6000 s). By combining Eq. (13) into one single equation of higher order, we obtain

$$\ddot{X} + (\omega_{\text{orb}}^2 + 2\omega_n^2)\dot{X} + \omega_n^2(\omega_n^2 - 3\omega_{\text{orb}}^2)X = 0, \quad (14)$$

whose eigenvalues are:

$$\Lambda_{1,2,3,4} = \pm i \sqrt{\omega_n^2 + \omega_{\text{orb}}^2/2 \mp 2\omega_{\text{orb}}\omega_n \sqrt{1 + \omega_{\text{orb}}^2/(16\omega_n^2)}}. \quad (15)$$

These eigenvalues give the angular frequencies of tidal effects in the reference frame of the satellite which orbits around the Earth at  $\omega_{\text{orb}}$ . For the EP experiments in space it is  $\omega_n \gg \omega_{\text{orb}}$ , and these frequencies become:

$$\Lambda_{1,2,3,4} = \pm i(\omega_n \pm \omega_{\text{orb}}). \quad (16)$$

If seen in the inertial reference frame (centered on the center of mass of the Earth and fixed in space), tidal effect would therefore appear at frequencies:

$$\nu_n, \quad \nu_n \pm 2\nu_{\text{orb}} \quad (17)$$

( $\nu = \omega/2\pi$ ). Hence, the effect of coupling the test masses in the orbit plane is to shift the tidal signal from the orbital frequency  $\nu_{\text{orb}}$  of the uncoupled case (see Fig. 3), to the (typically much larger) natural differential frequency  $\nu_n$  introduced by the coupling. What about the effect of coupling on an EP violation signal?

In order to answer this question we consider  $\eta \neq 0$  in the Lagrange function (12) and find that in this case there exists a position of relative equilibrium of the test masses in the Earth-to-satellite direction (the  $x$  axis of the

orbiting reference frame). The coordinates of the test masses at equilibrium are:

$$\begin{cases} r_{1x}^0 = \frac{\omega_n^2 r \eta}{6(\omega_n^2 - 3\omega_{\text{orb}}^2) + 2\eta(\omega_n^2 - 6\omega_{\text{orb}}^2)}, \\ r_{2x}^0 = r_{1x}^0 \left(1 - 6\frac{\omega_{\text{orb}}^2}{\omega_n^2}\right), \\ r_{1y}^0 = r_{2y}^0 = r_{1x}^0 \left(\frac{\omega_n^2}{\omega_n^2 + 2\eta\omega_{\text{orb}}^2}\right). \end{cases} \quad (18)$$

Since the equilibrium position (18) due to an EP violation  $\eta$  is fixed in the orbit plane of the reference frame of the orbiting satellite, it is apparent that in the inertial reference system the EP violation signal is at the orbital frequency (as in the case of uncoupled test masses), while tides are now close to the natural differential frequency due to coupling. Since the orbital frequency is several times lower than the natural one, we conclude that—thanks to coupling in the orbit plane—an EP violation signal can be well separated from classical tidal effects.

#### 4. Signal modulation

For high accuracy EP tests in space the spacecraft should also rotate, so as to modulate the signal at its rotation frequency relative to the Earth (the synodic frequency). EP tests require weak suspensions and large rotation rates: weak suspensions increase the sensitivity of the test masses to applied forces; fast rotation provides high frequency modulation and reduced “ $1/f$ ” noise. Conceptually, the problem is that of a rotating oscillator made of a body of mass  $m$  whose center of mass is suspended with stiffness  $k$  from a point located a vector  $\vec{\varepsilon}$  away from the rotation axis.  $\vec{\varepsilon}$  is the inevitable offset due to construction and mounting errors, and is fixed with the rotor. Two frequencies are relevant for equilibrium: the spin frequency  $\omega_s$  and the natural frequency  $\omega_n = \sqrt{k/m}$ . Equilibrium is achieved at a position  $\vec{r}_{\text{eq}}$  where the centrifugal force is balanced by the restoring force of the suspension:

$$\vec{r}_{\text{eq}} = \frac{1}{1 - (\omega_s/\omega_n)^2} \cdot \vec{\varepsilon}. \quad (19)$$

If  $\omega_s/\omega_n < 1$  (“sub-critical” rotation),  $\vec{r}_{\text{eq}} \parallel \vec{\varepsilon}$  and  $r_{\text{eq}} > \varepsilon$ : the equilibrium position moves farther away from the rotation axis than the original offset. If  $\omega_s/\omega_n > 1$  (“super-critical” rotation),  $\vec{r}_{\text{eq}} \parallel -\vec{\varepsilon}$  and  $|\vec{r}_{\text{eq}}| < |\vec{\varepsilon}|$ : equilibrium is achieved on the opposite side of the rotation axis with respect to  $\vec{\varepsilon}$  and closer to it than obtained by construction. Note that in this case equilibrium is not possible if the body is constrained to motion in one dimension, as it was demonstrated long time ago in Chapter 6 of [7]. If, moreover,

$$\frac{\omega_s^2}{\omega_n^2} \gg 1 \quad (20)$$

as it is desirable for very accurate EP tests, then:

$$\vec{r}_{\text{eq}} \simeq -\vec{\varepsilon} \frac{\omega_n^2}{\omega_s^2} \quad (21)$$

and self-centering occurs since the original offset is reduced by the large factor  $\omega_s^2/\omega_n^2 \gg 1$ . The same line of reasoning holds for two rotating coupled masses, whose relative position at equilibrium is as in (19),  $\omega_n$  now being the frequency of differential oscillations. This is the case of the GG experiment design, for which tidal effects and EP violation signal are analyzed in detail in Section 5. Note that, since the offset vector  $\vec{\varepsilon}$  is fixed with the rotor, the position vector of relative equilibrium is also fixed with the rotor, and therefore the corresponding tidal effect is (in the rotating reference frame) at twice the spin frequency, just as lunisolar tides on the surface of the Earth have periodicities of 12 h (solar tide) and 12 h 25 min (lunar tide).

## 5. EP violation signal and tidal effects in the GG space experiment design

Let us now analyze EP violation signal and tidal effects in the case of the GG experiment in space.

### 5.1. The GG apparatus

The GG satellite is planned to fly at an altitude of about 520 km on a circular sunsynchronous orbit around the Earth with inclination  $I = 97.494$  degrees (see [8]). The satellite spins around its symmetry axis at a rather high frequency (2 Hz with respect to the center of the Earth) and this rotation provides passive stabilization of the spacecraft attitude because the axis of symmetry is also the axis of maximum moment of inertia. Because of the flattening of the Earth, the orbit plane of an inclined satellite is known to precess around the normal to the Equator; in sunsynchronous orbits inclination and orbital radius are chosen so that the orbit plane follows the Sun in its annual motion around the Earth (at about  $1^\circ$  per day). Since the spin axis of GG remains fixed in space (due to the very high energy of spin), the angle  $\theta$  that separates it from the orbit normal will also increase by about  $1^\circ$  per day. In GG  $\theta$  is maintained within  $\pm 10^\circ$ , allowing about 20 days duration for each experiment run before realignment of the spin axis along the orbit normal is performed.

The test masses—referred to with subindexes 1 and 2—are two concentric, coaxial hollow cylinders, with the axes along the spin/symmetry axis of the spacecraft and weighing 10 kg each (planned to be made of Pt/Ir and CuBe). They are coupled as in a beam balance by means of mechanical suspensions which are stiff along the spin axis but very soft in the orthogonal plane, where high sensitivity to differential accelerations has to be provided. The mechanical suspensions also allow electric grounding of the test masses, so that no discharging mechanism is required (which would disturb the experiment).

Note that:  $\nu_s = \omega_s/2\pi = 2.000175$  Hz is the spin frequency of the satellite around its symmetry axis with respect to a star fixed reference frame;  $\nu_{\text{orb}} = \omega_{\text{orb}}/2\pi = 1.75 \times 10^{-4}$  Hz is the orbital frequency around the Earth and  $\nu_{\text{prec}} = \Omega_{\text{prec}}/2\pi = 3.17 \times 10^{-8}$  Hz is the frequency of precession of the normal to the orbit around the normal to the equator (too small to be detected in 20 days of integration time).

### 5.2. Whirl motion and tidal frequencies in the sensitive plane

In super-critical regime mechanical suspensions are known to undergo deformations (and therefore to dissipate energy) at the spin frequency. Energy dissipation makes the spin rate to decrease, together with the spin angular momentum. Since the total angular momentum must be conserved, the bodies develop a whirl motion of increasing amplitude around each other at a frequency close to the natural differential one due to the coupling. The smaller the losses (i.e., the higher the quality factor  $Q$ ), the slower is the growth rate of the whirl. GG relies on high  $Q$  (for slow growth) and on active whirl damping (see [9,10, Chapter 6]).

We use a simplified model, as sketched in Fig. 4 and write the equations of motion in the inertial reference frame  $(X, Y, Z)$  centered on the center of the Earth, the  $X$ -axis along the nodal line of the satellite's orbit at initial time, the  $Y$ -axis perpendicular to it in the orbit plane at initial time and the  $Z$ -axis along the spin axis, coinciding with the orbit normal at initial time.  $\vec{p}_1 = (x_1, y_1, 0)$  and  $\vec{p}_2 = (x_2, y_2, 0)$  are position vectors of the test masses with respect to the center of mass of the Earth while the satellite orbits around it with a constant radius  $r$ . The bodies have the same inertial mass but different composition, and there is a violation of equivalence to the level  $\eta$ , namely:  $m_1^i = m_2^i \equiv m$  and  $m_1^g = m$ ,  $m_2^g = m(1 + \eta)$ . They are coupled to each other by a dissipative spring with elastic constant  $k$  and quality factor  $Q$ . An offset vector  $\vec{\varepsilon} = \varepsilon(\cos(\omega_s t + \phi), \sin(\omega_s t + \phi), 0)$ , due to construction and mounting, locates the suspension point of the spring with respect to the center of mass of body 2; it is fixed with the rotor, and therefore spins with angular frequency  $\omega_s$  in the inertial reference frame. The dissipative force is proportional to the relative velocity through the coefficient  $c_r = k/Q\omega_s$  (sub-index “ $r$ ” stands for “rotating friction”, since it is determined by losses in the rotor).

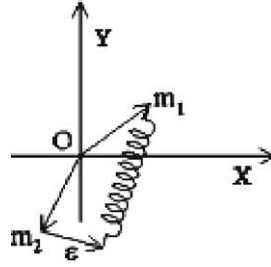


Fig. 4. Simplified model of the GG coupled test masses. The reference system is centered on the center of mass of the Earth; the  $X$ -axis is the line of nodes of the satellite orbit at initial time;  $(X, Y)$  is the orbit plane of the satellite at initial time; the  $Z$ -axis (not shown) is the spin axis, coinciding with the orbit normal at initial time;  $m_1$  and  $m_2$  are the test bodies, connected by a spring, with position vectors  $\vec{\rho}_1$  and  $\vec{\rho}_2$  from the center of mass of the Earth. The offset error due to inevitable construction and mounting imperfections is indicated as  $\varepsilon$ . The figure is obviously not to scale.

The equations of motion are:

$$\begin{aligned}\ddot{\vec{\rho}}_1 &= \frac{k}{m}(\vec{\rho}_2 - \vec{\rho}_1 + \vec{\varepsilon}) - \frac{c_r}{m}(\dot{\vec{\rho}}_1 - \dot{\vec{\rho}}_2 - \omega_s \times (\vec{\rho}_1 - \vec{\rho}_2)) - \frac{GM\vec{\rho}_1}{|\vec{\rho}_1|^3}, \\ \ddot{\vec{\rho}}_2 &= -\frac{k}{m}(\vec{\rho}_2 - \vec{\rho}_1 + \vec{\varepsilon}) + \frac{c_r}{m}(\dot{\vec{\rho}}_1 - \dot{\vec{\rho}}_2 - \omega_s \times (\vec{\rho}_1 - \vec{\rho}_2)) - \frac{GM\vec{\rho}_2(1 + \eta)}{|\vec{\rho}_2|^3},\end{aligned}\quad (22)$$

which we have integrated numerically with initial conditions:

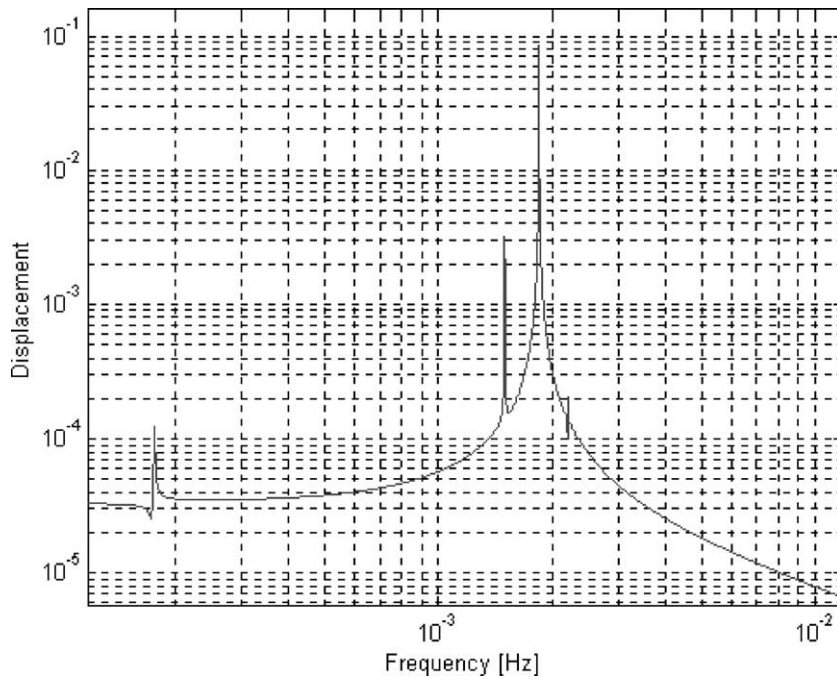
$$\begin{aligned}\vec{\rho}_1(0) &= (r + x_0, 0), & \dot{\vec{\rho}}_2(0) &= (r - x_0, 0), \\ \dot{\vec{\rho}}_1(0) &= (0, \omega_{\text{orb}}r + \sqrt{k/m}x_0), & \vec{\rho}_2(0) &= (0, \omega_{\text{orb}}r - \sqrt{k/m}x_0)\end{aligned}\quad (23)$$

representing a system in which whirl radius  $r_w = 2x_0$  at initial time. ( $\omega_n = \sqrt{k/m}$  is the natural differential frequency of the coupling.) For demonstration purposes the numerical integration is carried out with a very large whirl radius  $r_w = 2.5 \times 10^{-4}$  m and assuming a very high level of violation  $\eta = 10^{-11}$ . Instead, the natural differential period of the coupling (also the whirl period) is  $T_w = 540$  s as in GG, the quality factor is  $Q = 20000$  as originally assumed in GG (though better values have been measured), and  $\varepsilon = 10^{-6}$  m. Since at this point we are interested only in frequencies much faster than the precession frequency, the numerical integration timespan is short and precession is not included.

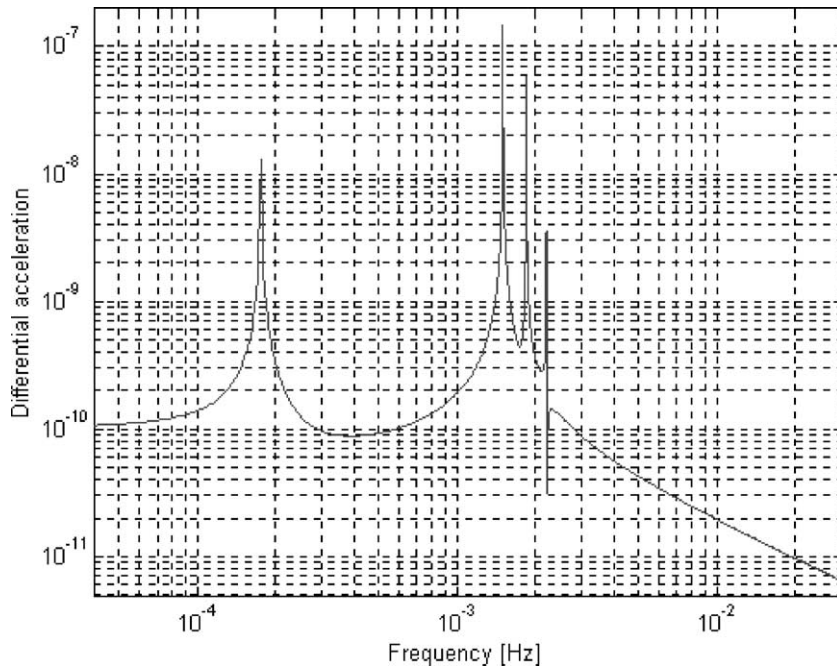
The resulting FFT of the relative displacement between the test bodies is shown in Fig. 5(a) where all four expected peaks are visible: whirl motion appears at  $\nu_w = 0.00185$  Hz  $\approx \nu_n$ , tidal effect at  $\nu_w$ ,  $\nu_w + 2\nu_{\text{orb}} = 0.00220$  Hz,  $\nu_w - 2\nu_{\text{orb}} = 0.00150$  Hz and EP signal at  $\nu_{\text{orb}} = 0.000175$  Hz (EP signal has a peak at  $\nu_s$  too due to the offset). The FFT of the relative acceleration between the test masses is plotted in Fig. 5(b).

We now derive the same results by analytical methods, taking into account also precession. Let  $(s_1, s_2, s)$  be a reference frame fixed with the satellite, where  $s$  is in the direction of the spin axis (coinciding with the orbit normal  $Z$  at initial time),  $s_1$  is along the nodal line at initial time (same as  $X$ -axis) and  $(s_1, s_2)$  is therefore the sensitive plane of the instrument. In the reference system identified by the equatorial plane of the Earth and by its rotation axis it is:  $s_1 = (1, 0, 0)$ ,  $s_2 = (0, \sin I, \cos I)$  and  $s = (0, -\sin I, \cos I)$  and the unit position vector of the satellite at time  $t$  is:

$$\hat{r} = \cos(\omega_{\text{orb}}t + \varphi) \begin{pmatrix} \cos(\Omega_{\text{prec}}t) \\ \sin(\Omega_{\text{prec}}t) \\ 0 \end{pmatrix} + \sin(\omega_{\text{orb}}t + \varphi) \begin{pmatrix} -\cos(I) \sin(\Omega_{\text{prec}}t) \\ \cos(I) \cos(\Omega_{\text{prec}}t) \\ \sin(I) \end{pmatrix}, \quad (24)$$



(a)



(b)

Fig. 5. (a) FFT of the relative displacement where all four expected peaks are visible, which are assigned to whirl motion at  $\nu_w = 0.00185 \text{ Hz} \approx \nu_n$ , to the tidal effect at  $\nu_w$ ,  $\nu_w + 2\nu_{\text{orb}} = 0.00220 \text{ Hz}$ ,  $\nu_w - 2\nu_{\text{orb}} = 0.00150 \text{ Hz}$  and to an EP violation signal at  $\nu_{\text{orb}} = 0.000175 \text{ Hz}$ . (b) FFT of the relative acceleration in the presence of an EP violation to the level  $\eta = 10^{-11}$ , which is sensed at  $\nu_{\text{orb}}$ , while whirl motion is at  $\nu_w$  and tides are at  $\nu_w$  and  $\nu_w \pm 2\nu_{\text{orb}}$ .

Table 1

Tidal acceleration components in the sensitive plane of the GG system

Component	Frequency
$\frac{GM_{\oplus}}{r^3} 3r_w e^{\omega_w t / (2Q)} \cos(\omega_w t) \cos^2(\omega_{\text{orb}} t) \cos^2(\Omega_{\text{prec}} t)$	$\omega_w, \omega_w \pm 2\omega_{\text{orb}} \pm 2\Omega_{\text{prec}}$
$\frac{GM_{\oplus}}{r^3} \frac{3}{2} r_w e^{\omega_w t / (2Q)} \sin^2(I) \sin(\omega_w t) \sin(2\omega_{\text{orb}} t) \cos(\Omega_{\text{prec}} t)$	$\omega_w \pm 2\omega_{\text{orb}}, \omega_w \pm 2\Omega_{\text{prec}}$
$-\frac{GM_{\oplus}}{r^3} r_w e^{\omega_w t / (2Q)} \cos(\omega_w t)$	$\omega_w$
$\frac{GM_{\oplus}}{r^3} 3r_w \sin^2(I) \cos(I) e^{\omega_w t / (2Q)} \sin(\omega_w t) \sin^2(\omega_{\text{orb}} t) \sin(\Omega_{\text{prec}} t)$	$\omega_w \pm \Omega_{\text{prec}}, \omega_w \pm 2\omega_{\text{orb}} \pm 2\Omega_{\text{prec}}$
$\frac{GM_{\oplus}}{r^3} \frac{3}{2} r_w \cos(I) e^{\omega_w t / (2Q)} \sin(\omega_w t) \cos^2(\omega_{\text{orb}} t) \sin(2\Omega_{\text{prec}} t)$	$\omega_w \pm 2\Omega_{\text{prec}}, \omega_w \pm 2\omega_{\text{orb}} \pm 2\Omega_{\text{prec}}$
$-\frac{GM_{\oplus}}{r^3} \frac{3}{2} r_w \cos(I) e^{\omega_w t / (2Q)} \cos(\omega_w t) \sin(2\omega_{\text{orb}} t) \sin(2\Omega_{\text{prec}} t)$	$\omega_w \pm 2\omega_{\text{orb}} \pm 2\Omega_{\text{prec}}$
$\frac{GM_{\oplus}}{r^3} \frac{3}{2} r_w \cos^2(I) e^{\omega_w t / (2Q)} \sin(\omega_w t) \sin(2\omega_{\text{orb}} t) \cos(2\Omega_{\text{prec}} t)$	$\omega_w, \omega_w \pm 2\omega_{\text{orb}} \pm 2\Omega_{\text{prec}}, \omega_w \pm 2\Omega_{\text{prec}}, \omega_w \pm 2\omega_{\text{orb}}$
$\frac{GM_{\oplus}}{r^3} \frac{3}{2} r_w \cos^2(I) e^{\omega_w t / (2Q)} \cos(\omega_w t) \sin^2(\omega_{\text{orb}} t) \sin^2(\Omega_{\text{prec}} t)$	$\omega_w \pm 2\omega_{\text{orb}} \pm 2\Omega_{\text{prec}}$
$\frac{GM_{\oplus}}{r^3} \frac{3}{2} r_w \cos^3(I) e^{\omega_w t / (2Q)} \sin(\omega_w t) \sin^2(\omega_{\text{orb}} t) \sin(2\Omega_{\text{prec}} t)$	$\omega_w \pm 2\Omega_{\text{prec}}, \omega_w \pm 2\omega_{\text{orb}} \pm 2\Omega_{\text{prec}}$

while whirl motion is described by the vector

$$\vec{p} = r_w e^{\frac{\omega_w t}{2Q}} \begin{pmatrix} \cos(\omega_w t) \\ \sin(\omega_w t) \cos(I) \\ \sin(\omega_w t) \sin(I) \end{pmatrix}. \quad (25)$$

Then, the tidal (differential) acceleration between the test bodies is:

$$\vec{a} = -\frac{GM}{r^3} \left\{ -3r_w e^{\frac{\omega_w t}{2Q}} \sin(\omega_w t) [(\hat{r} \times \hat{s}) \cdot \hat{s}_1] \hat{r} - 3r_w e^{\frac{\omega_w t}{2Q}} \cos(\omega_w t) (\hat{r} \cdot \hat{s}_1) \hat{r} + \vec{p} \right\} \quad (26)$$

and its components in the sensitive plane are:

$$\begin{aligned} a_{s1} &= \vec{a} \cdot \hat{s}_1 = -\frac{GM}{r^3} \left\{ -3r_w e^{\frac{\omega_w t}{2Q}} \sin(\omega_w t) [(\hat{r} \times \hat{s}) \cdot \hat{s}_1] (\hat{r} \cdot \hat{s}_1) - 3r_w e^{\frac{\omega_w t}{2Q}} \cos(\omega_w t) (\hat{r} \cdot \hat{s}_1)^2 + \vec{p} \cdot \hat{s}_1 \right\}, \\ a_{s2} &= \vec{a} \cdot \hat{s}_2 = -\frac{GM}{r^3} \left\{ -3r_w e^{\frac{\omega_w t}{2Q}} \sin(\omega_w t) [(\hat{r} \times \hat{s}) \cdot \hat{s}_1] (\hat{r} \cdot \hat{s}_2) - 3r_w e^{\frac{\omega_w t}{2Q}} \cos(\omega_w t) (\hat{r} \cdot \hat{s}_2) (\hat{r} \cdot \hat{s}_1) + \vec{p} \cdot \hat{s}_2 \right\}. \end{aligned} \quad (27)$$

Using (24) in (27) we can list all the frequencies at which the whirl-related tides take place. Acceleration  $a_{s1}$  can be seen as the sum of the nine signals listed in Table 1. The same holds for  $a_{s2}$ .

The table shows that tides between the test masses occur at angular frequencies  $\omega_w, \omega_w \pm 2\omega_{\text{orb}}, \omega_w \pm 2\Omega_{\text{prec}}, \omega_w \pm 2\omega_{\text{orb}} \pm 2\Omega_{\text{prec}}$ , and  $\omega_w \pm 2\omega_{\text{orb}} \pm \Omega_{\text{prec}}$ . In the case of GG, however,  $\Omega_{\text{prec}}$  is too tiny to be detected. Thus, the relevant frequencies of the tides in GG are  $\omega_w$  and  $\omega_w \pm 2\omega_{\text{orb}}$ , in agreement with the numerical simulation.

We conclude this analysis by showing in Fig. 6 the time evolution of the EP violation signal component  $a_{s1}^{\text{EP}} = -(GM_{\oplus}/r^3)\eta(\vec{r} \cdot \hat{s}_1)$  as compared to the same component of the tidal effect, giving the corresponding FFT analysis in Fig. 7. It is apparent that the wide separation in frequency allows an EP violation signal to be recovered even if it is much smaller than tidal effects.

### 5.3. Tides due to relative displacements along the spin/symmetry axis

Even if the GG system is stiff along the spin/symmetry axis Z, perturbations acting along this direction are present (e.g., due to solar radiation pressure or to coupling of the Earth's monopole with higher mass moments of the test bodies) which may produce a displacement between the centers of mass of the test cylinders. Unless the spin axis remains all time exactly perpendicular to the orbit plane (which is not the case in GG), a center of mass separation along its direction will give a tidal signal also in the sensitive plane. We use the same analytical

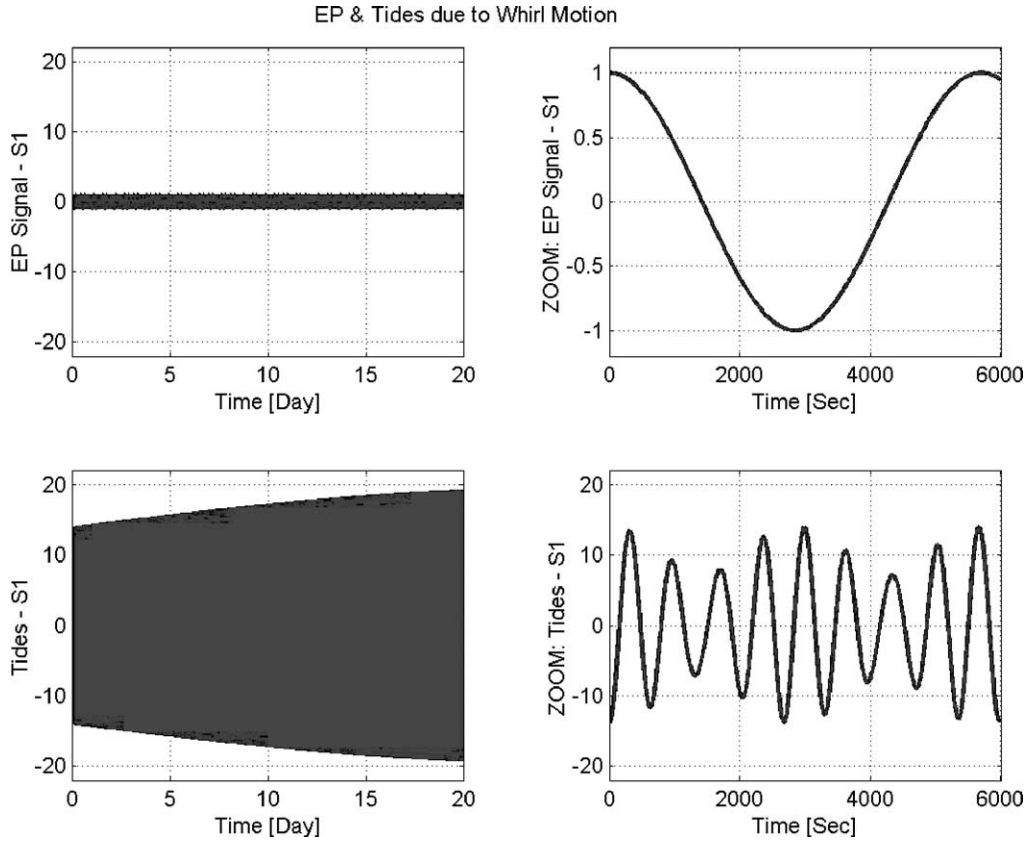


Fig. 6. Time evolution of the EP violation signal (above) and of the tidal signal (below) along the  $s_1$  direction in the sensitive plane. All signals are given in units of  $(GM_{\oplus}/r^2) \cdot \eta = 1$ .

procedure as in Section 5.2 to describe the resulting tidal signal. The tidal acceleration  $\vec{a}$  corresponding to the relative separation vector  $(0, 0, \Delta z)$  with respect to the satellite center-of-mass, can be written as

$$\vec{a} = -\frac{1}{2} \frac{GM_{\oplus}}{r^3} \Delta z \hat{s} + \frac{3}{2} \frac{GM_{\oplus}}{r^3} \Delta z \hat{r} (\hat{r} \cdot \hat{s}). \quad (28)$$

In the reference frame  $(s_1, s_2, s)$ , we have

$$\begin{aligned} a_{s1} &= \frac{3}{2} \frac{GM_{\oplus}}{r^3} \Delta z r_x (r_y \sin(I) - r_z \cos(I)), \\ a_{s2} &= \frac{3}{2} \frac{GM_{\oplus}}{r^3} \Delta z \left[ \frac{1}{2} (r_y^2 - r_z^2) \sin(2I) - r_y r_z \cos(2I) \right]. \end{aligned} \quad (29)$$

The corresponding time evolution and FFT analysis are reported in Figs. 8 and 9. In this case, tidal effects are detected at frequency  $2\nu_{\text{orb}}$ , while the EP signal is still at  $\nu_{\text{orb}}$ . The peak at  $2\nu_{\text{orb}}$  in Fig. 9 does not resolve the contributions at  $2\nu_{\text{orb}} \pm \nu_{\text{prec}}$  and  $2\nu_{\text{orb}} \pm 2\nu_{\text{prec}}$ .

We end this section noticing that, although the frequency analysis of tidal effects is useful in order to understand the physical nature of these subtle perturbations, in the actual GG experiment the measurement data provided by the capacitance bridges, rotating with the test cylinders and the whole spacecraft at a nominal frequency of 2 Hz, are transformed (using the reference signal provided by the Earth elevation sensor onboard the spacecraft) into an Earth pointing, non-rotating reference frame centred in the centre of mass of the spacecraft. In this frame an

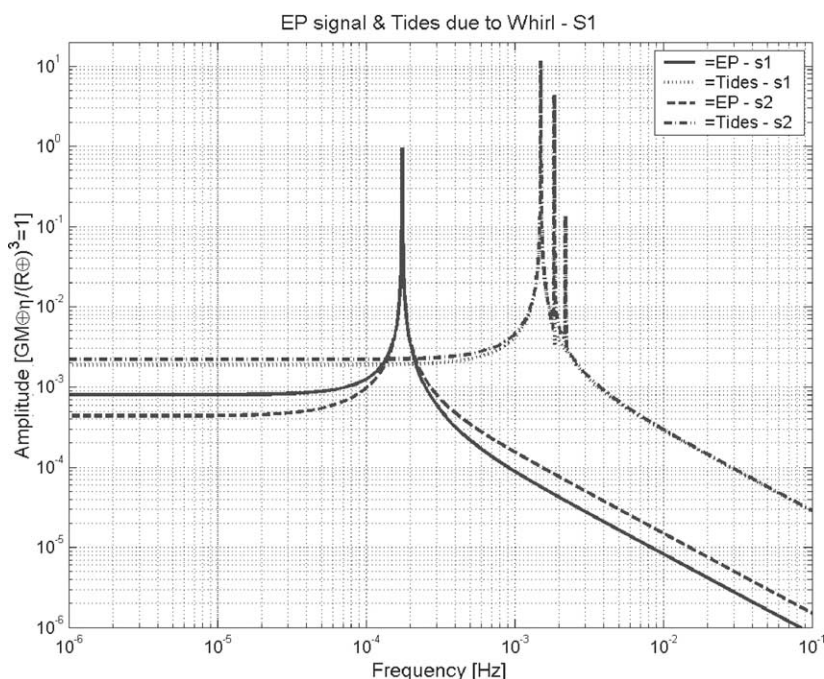


Fig. 7. FFT analysis of the data shown in Fig. 6. The amplitudes of the tidal peaks are about 20 times larger than the EP signal. Nevertheless, the differences between the orbital and the whirl frequency allows us to recover the EP signal from the FFT analysis.

EP violation signal appears as a constant offset (for zero orbital eccentricity) in the satellite-to-Earth direction while tidal disturbances appear at a frequency close to the natural differential frequency of the test cylinders, and therefore average out to zero.

## 6. EP violation signal and tidal effects with test masses coupled and controlled in one dimension: the STEP and $\mu$ SCOPE cases

In STEP and  $\mu$ SCOPE the test cylinders are sensitive only along the symmetry axis, which lies and rotates (in order to modulate the signal) in the orbital plane. Being constrained to motions in 1D the test bodies are bound to sub-critical rotation, with no self-centering (see Section 4). Sub-critical rotation is indeed confirmed for STEP by the values of the rotation and oscillation frequencies reported in [11]. Since the original offset  $\varepsilon$  can hardly be smaller than 1  $\mu\text{m}$ , the residual tidal acceleration would exceed the signal by orders of magnitude. Furthermore, the center-of-mass separation—hence the tidal effect—are not exactly constant because radial oscillations, in the plane perpendicular to the sensitive axis, are excited by residual spacecraft motion. Thus, a component of the large tidal disturbance would appear at the signal frequency as well. This is why tides must be reduced, i.e., the masses must be actively centered.

Let us therefore calculate this control force, assuming no spacecraft rotation at first. In the inertial reference frame  $(X, Y, Z)$  centered on the center of mass of the Earth the satellite orbits in the  $(X, Y)$  plane and its position vector is  $\vec{r} = r(\cos(\omega_{\text{orb}}t), \sin(\omega_{\text{orb}}t), 0)$ . For simplicity, the first test mass is assumed to coincide with the center of mass of the satellite, while the second one is separated from it by the vector  $\Delta\vec{r} = \Delta r \hat{X}$  along the  $X$  direction. A force equal and opposite to the tidal one must be applied in order to maintain the second mass fixed in its position.

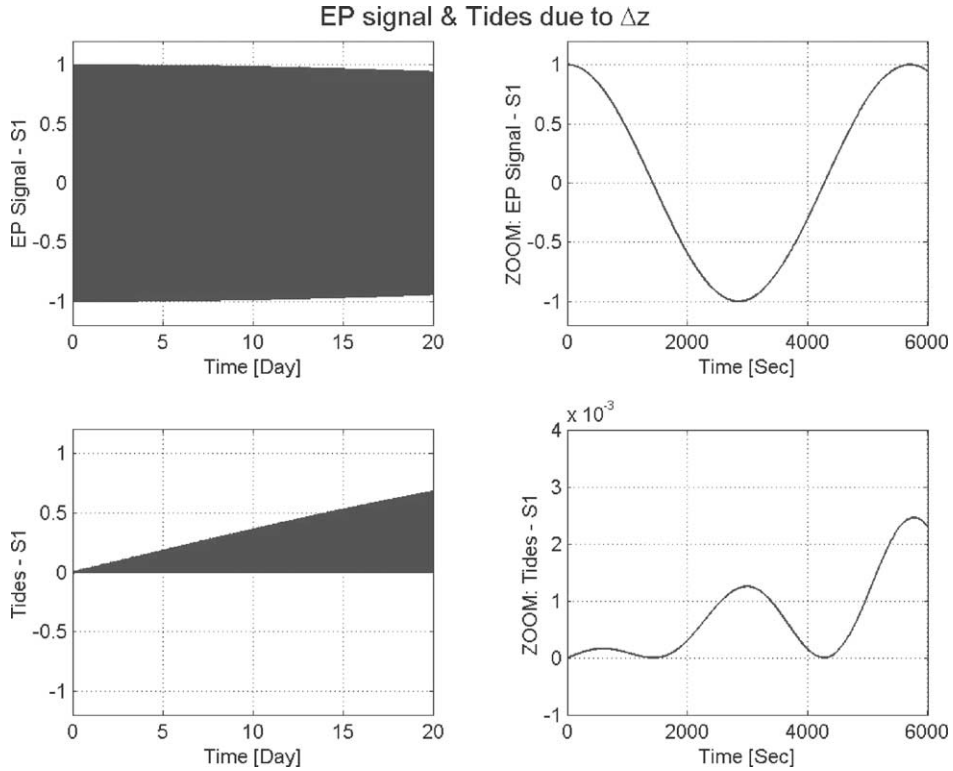


Fig. 8. Time evolution of the EP signal (above) and tidal signal due to a center of mass offset along the spin axis (below) in the  $s_1$  direction of the sensitive plane. All signals are given in units of  $(GM_{\oplus}/r^2) \cdot \eta = 1$ .

The tidal force to be reduced to zero is:

$$\vec{F}_2^{\text{Tide}} = -GMm \left( \frac{\vec{r} + \Delta\vec{r}}{|\vec{r} + \Delta\vec{r}|^3} - \frac{\vec{r}}{r^3} \right) = -\frac{GMm}{r^3} \left( \Delta\vec{r} - 3\frac{\vec{r}\Delta\vec{r}}{r^2} \cdot \vec{r} \right) = -m\omega_{\text{orb}}^2 \left( \Delta\vec{r} - 3\frac{\vec{r}\Delta\vec{r}}{r^2} \cdot \vec{r} \right) \quad (30)$$

or else, after making the time-dependence explicit,

$$\vec{F}_2^{\text{Tide}} = -m\omega_{\text{orb}}^2 \left[ \Delta r (1 - 3\cos^2(\omega_{\text{orb}}t)), -\frac{3}{2}\Delta r \sin(2\omega_{\text{orb}}t), 0 \right]. \quad (31)$$

It is apparent from (31) that the tidal force, as well as the control force required to make it vanish, are at the frequency  $2\nu_{\text{orb}}$  in the inertial reference frame.

Let us now assume that the test masses are perfectly coincident, while there is an EP violation such that  $m_2 = m(1 + \eta)$ . In this case the control force required to maintain the second mass fixed is equal and opposite to the EP violation force

$$\vec{F}_2^{\text{EP}} = -\frac{GMm}{r^3} \eta \vec{r} = -m\omega_{\text{orb}}^2 \eta \vec{r}, \quad (32)$$

which is at frequency  $\nu_{\text{orb}}$ . In this case too, as in GG, we can distinguish the tidal effect from the EP violation. However, typical orbital periods of the spacecraft are of the order of 6000 s, resulting in a separation as small as  $1.7 \times 10^{-4}$  Hz in the FFT spectrum. In STEP and  $\mu$ SCOPE too the spacecraft spins in order to modulate the signal. Note, however, that the rotation axis is not the symmetry axis of the test cylinders—which is the sensitive axis—but is perpendicular to it. After demodulation of the output signal (i.e., in the non-rotating reference frame), the EP

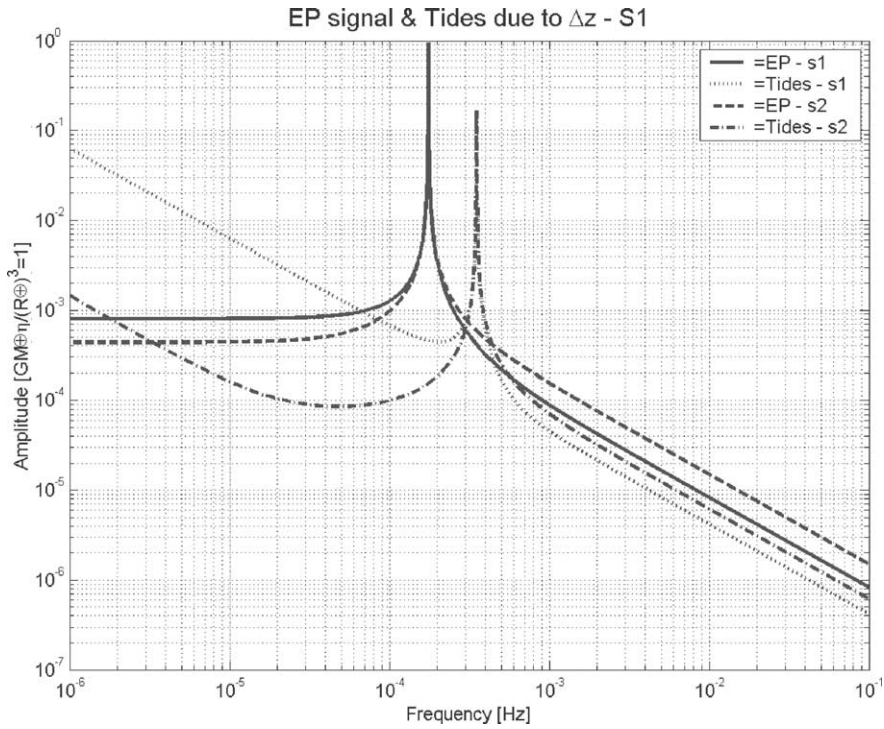


Fig. 9. FFT analysis of the data shown in Fig. 8. For a center of mass separation along the spin axis tidal effects appear in the sensitive plane at frequency  $2\nu_{\text{orb}}$ , while the EP signal is still at  $\nu_{\text{orb}}$ .

violation signal is still at the orbit frequency  $\nu_{\text{orb}}$ , as it is apparent from (32), where the position satellite-to-Earth vector  $\vec{r}$  is obviously unaffected by the rotation of the spacecraft. Instead, the tidal force (30) contains the relative position vector  $\Delta\vec{r}$  between the test masses, which rotates with the spacecraft at its spin angular frequency  $\omega_s$ . Its coordinates in the non-rotating frame are:

$$\Delta\vec{r} = \Delta r (\cos(\omega_s t), \sin(\omega_s t), 0) \quad (33)$$

and the tidal force becomes:

$$\vec{F}_2^{\text{Tide}} = \frac{1}{2} m \omega_{\text{orb}}^2 \Delta r [(\cos(\omega_s t) + 3 \cos((\omega_s - 2\omega_{\text{orb}})t)), (\sin(\omega_s t) - 3 \sin((\omega_s - 2\omega_{\text{orb}})t)), 0] \quad (34)$$

thus showing that tides are (in the non-spinning frame) at frequencies  $\nu_s$  and  $2\nu_s - \nu_{\text{orb}}$ . This means that they can be separated from the EP violation signal at frequency  $\nu_{\text{orb}}$ ; however, if the spacecraft rotates slowly (with a spin period not much smaller than the orbital one) as it is the case in STEP and  $\mu\text{SCOPE}$  the separation in frequency between the two is still small, and due to the difficulties of active centering, the residual tide is still much larger than the target signal. It is also worth noticing that, in this design in which the test masses are actively forced to remain in a fixed relative position, the observable from which a possible EP violation signal can be extracted is the control force equal and opposite to the differential force of an EP violation. However, the latter is in the form (32) if the test masses are allowed to move in the orbital plane around the Earth. Instead, they are forced to move along one direction only (the symmetry axis) of this plane, while the suspension is very stiff in the other direction. How this stiff suspension does influence the motion (hence the control force) along the sensitive axis is a matter of concern for the STEP scientists (see [12,13]).

Electric charging of the test masses is a problem with electrostatic and magnetic suspensions. In  $\mu\text{SCOPE}$  a thin gold (conductive) wire is added to ground the masses [14], while the STEP masses need active discharging.

We end this section by noticing that a fixed relative position of the test masses could also be provided by gravitation only. This was suggested in [15] for a short distance EP test exploiting the Lagrangean equilateral configuration of equilibrium for a primary body and two test masses (of different composition) inside a high-altitude spacecraft. In this case a composition-dependent effect would show up as a deviation from the equilateral triangle of classical equilibrium.

## 7. Conclusions

Experiments to test the equivalence principle inside a spacecraft in low Earth orbit require classical tidal (differential) effects between the test masses to be separated from a non-classical differential signal due to a possible violation of equivalence. If the test bodies are free flying inside the spacecraft tidal effects have the same frequencies as an EP violation signal. However, if the initial conditions are adjusted until the test bodies reach a fixed configuration relative to each other while orbiting around the Earth, then only by measuring their relative displacement it would be possible to tell whether the equivalence principle is violated or not. The displacement measurement can be very accurate, but such a fixed configuration is hard to reach and to maintain due to non-gravitational forces, primarily the electrostatic forces caused by electric charging of the test bodies.

The frequencies of tides can be widely separated from the frequency of an EP violation signal by (weakly) coupling the test masses (concentric coaxial cylinders) in the orbit plane. In this case the signal is at the orbital frequency while tides are at the natural differential frequency of the coupling (several times larger than the orbital one) and at this frequency plus or minus twice the orbital frequency. If the spacecraft spins in order to modulate the signal, weak coupling in 2D allows (fast) rotation in super-critical regime around the symmetry axis of the cylinders. In this regime a self centered position of relative equilibrium exists by physical laws, and tidal effects due to whirl motion around it are again widely separated from the signal (the whirl frequency is very close to the natural differential frequency of the coupling). This is the GG experiment design.

If the test masses are weakly coupled in 1D tides are at twice the orbital frequency, i.e., a factor 2 away from the frequency of EP violation. However, when spinning the spacecraft for signal modulation 1D motion only allows (slow) rotation in sub-critical regime. In this regime the relative distance between the test masses at equilibrium would be far too large to be acceptable (it would produce too large tidal effects), and therefore they need to be centered actively, and to be maintained fixed in that configuration. During rotation tides are at the spin frequency and at the spin frequency minus twice the orbital one, which under this condition of slow rotation are close to each other. Tides are also larger than the signal due to the difficulties of active centering. This is the STEP and  $\mu$ SCOPE experiment design. Its limitations appear to derive from the fact that rotation is not along the symmetry axis of the test cylinders.

## Acknowledgements

We thank ASI (Agenzia Spaziale Italiana) for its support of the GG mission studies and INFN for funding the development of a laboratory prototype of the apparatus proposed for space.

## Appendix A

Let us start from Eq. (1) in Section 2.1, namely,  $a(1 - e) = r + \Delta r$ .

The angular momentum per unit mass  $J$  is expressed as

$$J^2 = GM_{\oplus}a(1 - e^2) \tag{A.1}$$

and is a conserved quantity, so that

$$J^2 = J^2(0) = r_2^2(0)v_2^2(0) = GM_{\oplus}r \left(1 + \frac{\Delta r}{r}\right)^2. \quad (\text{A.2})$$

By equating (A.1) and (A.2), it follows:

$$a = \frac{r(1 + \Delta r/r)^2}{1 - e^2}. \quad (\text{A.3})$$

Eliminating  $a$  from (1) and (A.3) we obtain the exact expression

$$e = \frac{\Delta r}{r} \quad (\text{A.4})$$

for the eccentricity of body 2, valid to any order in  $\Delta r/r$ .

After substituting (A.4) into (A.3) and expanding to second order in  $\Delta r/r$ , the major semiaxis turns out to be

$$a = r \frac{1 + \Delta r/r}{1 - \Delta r/r} \simeq r \left(1 + 2\frac{\Delta r}{r} + 2\frac{\Delta r^2}{r^2}\right). \quad (\text{A.5})$$

The mean anomaly  $n_2$  is obtained from Kepler's third law, namely:

$$n_2^2 a^3 = GM_{\oplus} \quad (\text{A.6})$$

with the major semiaxis given by (A.5). To first order in  $\Delta r/r$ ,

$$n_2 = \sqrt{\frac{GM_{\oplus}}{r^3}} \cdot \left(1 + 2\frac{\Delta r}{r}\right)^{-3/2} \simeq n_1 \cdot \left(1 - 3\frac{\Delta r}{r}\right) \quad (\text{A.7})$$

resulting in the difference  $\Delta n$

$$\Delta n \equiv n_2 - n_1 \simeq -n_1 \cdot \frac{3\Delta r}{r}. \quad (\text{A.8})$$

## Appendix B

In the case  $\eta \neq 0$ , Eq. (A.1) is modified into

$$J^2 = GM_{\oplus}(1 + \eta)a(1 - e^2), \quad (\text{B.1})$$

while the initial condition is  $J^2(0) = r_2^2(0)v_2^2(0) = GM_{\oplus}r$ . The energy per unit of inertial mass is instead

$$E = -\frac{GM_{\oplus}(1 + \eta)}{2a} \quad (\text{B.2})$$

and the eccentricity satisfies the relation

$$e^2 = 1 + \frac{2EJ^2}{G^2M_{\oplus}^2(1 + \eta)^2}. \quad (\text{B.3})$$

Finally, the Kepler's third law in Eq. (A.6) is changed into

$$n_2^2 a^3 = GM_{\oplus}(1 + \eta). \quad (\text{B.4})$$

Combining Eqs. (B.1)–(B.4), expanding to second order in  $\eta$  and retaining only the linear terms, we obtain the relations (6) of the main text.

## Appendix C

Eqs. (1) and (A.2) with the initial conditions (8) give us the exact expressions for the Keplerian elements for the orbit of body 2. These are

$$a = \frac{r(1 + \Delta r/r)^4}{1 - e^2} \quad (\text{C.1})$$

for the major semiaxis,

$$e = \left(1 + \frac{\Delta r}{r}\right)^3 - 1 \quad (\text{C.2})$$

for the eccentricity, and

$$n_2 = \sqrt{\frac{GM_\oplus}{(r + 4\Delta r)^3}} = n_1 \left(1 + 4\frac{\Delta r}{r}\right)^{-3/2} \quad (\text{C.3})$$

for the mean anomaly. After expansion of equations (C.1)–(C.3) to second order in  $\Delta r/r$ , we obtain

$$a \simeq r \left(1 + 4\frac{\Delta r}{r} + 18\frac{\Delta r^2}{r^2}\right), \quad e \simeq 3\frac{\Delta r}{r} + 6\frac{\Delta r^2}{r^2}, \quad \Delta n \simeq -n_1 \cdot \frac{6\Delta r}{r}. \quad (\text{C.4})$$

## References

- [1] A.M. Nobili, et al., “Galileo Galilei-GG”: design, requirements, error budget and significance of the ground prototype, “Galileo Galilei-GG” website: <http://eotvos.dm.unipi.it/nobili>.
- [2] STEP Satellite Test of the Equivalence Principle, 1996, report on the phase A study, ESA-SCI(96)5, STEP website: <http://einstein.stanford.edu/STEP>.
- [3] Microscope website:  
[http://www.cnes.fr/activites/connaissance/physique/microsatellite/1sommaire\\_microsatellite.htm](http://www.cnes.fr/activites/connaissance/physique/microsatellite/1sommaire_microsatellite.htm),  
<http://www.onera.fr/dmph-en/accelerometre>.
- [4] J.P. Blaser, *Class. Quantum Grav.* 18 (2001) 2509.
- [5] Y. Jafry, *Class. Quantum Grav.* 15 (1998) 1.
- [6] J. Anderson, J.G. Williams, *Class. Quantum Grav.* 18 (2001) 2447.
- [7] J.P. Den Hartog, *Mechanical Vibrations*, Dover, New York, 1985.
- [8] A. Anselmi, G. Catastini, Design of the GG satellite, in press.
- [9] S.H. Crandall, A.M. Nobili, On the Stabilization of the GG System (1997), available on line: <http://tycho.dm.unipi.it/nobili/ggweb/crandall>.
- [10] “Galileo Galilei” (GG), Phase A Report, (1998), 2nd Edition, Agenzia Spaziale Italiana, 2000, <http://eotvos.dm.unipi.it/nobili/ggweb/phaseA>.
- [11] J. Mester, et al., *Class. Quantum Grav.* 18 (2001) 2475.
- [12] J.P. Blaser, On the motion of the STEP masses, STEP Note (2000).
- [13] J.P. Blaser, Motion of a STEP mass with EP-violation, STEP Note (2001).
- [14] P. Touboul, M. Rodrigues, *Class. Quantum Grav.* 18 (2001) 2487.
- [15] A.M. Nobili, A. Milani, in: O. Fackler, Tran Thanh Van (Eds.), *Fifth Force and Neutrino Physics*, Edition Frontieres, 1998, p. 569.

**Errata corrige:**

Tidal effect in space experiments to test the equivalence principle: implications on the experiment design, Physics Letters A, 318, 251-269, 2003

Page 266, first line after Eq. (34):

$2\nu_s - \nu_{orb}$  should read  $\nu_s - 2\nu_{orb}$